Progress In Electromagnetics Research C, Vol. 119, 81–96, 2022

Full Duplex High Speed Data Transmission Based on Partially Coupled Coils in Wireless Power Transmission Systems

Jianxiong Li* **and Wenlong Yang**

Abstract—For full duplex communication, a signal parallel transfer method based on partial power transmission couplers is proposed in this paper. The power transfer uses a serial LC compensation structure topology, and the data transmission channel adopts a double coupling resonant circuit. In terms of power transmission, some power coupling inductors and power compensation capacitors form a power resonance network with a high frequency trap function, which can isolate the influence of signal transmission. Therefore, there is no need for an additional trap, which reduces power loss and the space occupied by the structure. In terms of signal transmission, the partial coupling coil method can increase the coupling frequency and data transfer rate. In addition, the signal transmission circuit has the characteristics of dual resonance frequencies. The forward and reverse signals modulate the carrier at different resonance frequencies to realize full duplex communication. Finally, the simulation results prove that the scheme is practicable for full duplex communication and parallel transmission of power achieving an output power of 1.4 KW, and the highest transmission rate can reach 1 Mbps.

1. INTRODUCTION

With the growing electronic technology, wireless power transmission (WPT) technology has already been applied in numerous fields due to its accessibility and reliability [1, 2]. In terms of safety, WPT technology can reduce wear and sparks. For mobile electrical equipment, inflammable and explosive hazardous environments, WPT technology is safer than wire power transmission; in terms of flexibility, WPT technology effectively eliminates the impact of equipment dependence on lines and increases flexibility of equipment, especially for vehicles, high-speed rail, and other transportation vehicles [3]; in terms of environmental protection, for some biological implantable devices, due to the liberation from the line bondage, WPT technology can avoid bacterial infection, so the safety is higher than traditional power supply methods. It has successful applications in robotics, biomedical equipment, and home appliances [4, 5].

For many such applications, reliable communication at both ends of the transfer coils is requisite to improve the stability and real-time performance of the system. For example, load detection and condition monitoring require stable communication with the WPT system [6]. It should be noted that in the existing data communication mode, WPT systems use the conventional technologies such as Bluetooth, ZigBee, RF, and wireless network to achieve two-party communication [7–10]. However, these techniques require complex pairs between the sender and receiver, and have relatively long transmitting delays. At the same time, the attenuation is strong in the harsh environment such as metal shielding and marine underwater environment, which is not conducive to the transmission of information and lack of the advantages energy wireless transmission. Moreover, these approaches need extra coils as well as antennas to transmit the information, leading to systematic complexities with high-cost [11]. In

Received 27 January 2022, Accepted 4 March 2022, Scheduled 22 March 2022

* Corresponding author: Jianxiong Li (lijianxiong@tiangong.edu.cn).

The authors are with the School of Electronic and Information Engineering, Tiangong University, Tianjin, China; Tianjin Key Laboratory of Optoelectronic Detection Technology and Systems, Tianjin, China.

addition, for some limited operating space, additional information transmission modules increase the size of the system and interfere with other coils. The power coupling coil with the advantages of strong anti-interference, good electromagnetic compatibility, simple system structure, and small size is adopted as the common channel of signal coupling coil to achieve the parallel transfer of electricity and signal. That decreases the disturbance to other coils and enhances the system integration. That has better development prospects [12–14].

In [15], the frequency shift keying (FSK) technique was applied to the control of the frequency of the power transfer. The power transfer efficiency is the same in each frequency, and the signal transmission is realized according to the voltage of the sampling resistor. However, this situation will produce a large amount of energy loss, and the receiving voltage of electric energy transmission will not stabilize at a value under the frequency. In [16], a single channel dual resonant circuit is used. One resonant point transmits electric energy, and one resonant point transmits signals, which can only realize half duplex communication. In [17], the communication signal and electric energy signal share a set of coupling mechanism, and the wave trap is used to separate the transmission topology of electric energy and information. That solves the mutual restriction between electric energy and information operating frequency. However, under this circuit structure, the communication rate will not be very high, and the wave trap needs to connect the energy circuit in series. Its losses have a significant influence on the electrical power transmission efficiency, as well as the size and economic cost of the system. Using all energy coupling coils as data transmission coils will result in a large high frequency impedance of the data transmission loop due to a relatively large inductance value, which will eventually lead to a relatively large attenuation of the high frequency data carrier. However, reducing the inductance of the energy coupling coil cannot meet the demand for power transmission.

In this paper, in order to construct a high-speed data transmission channel and ensure the normal transmission of electric energy, we propose a circuit topology based on a partial energy coupling coil as a signal transmission, and series-series (SS) topology as power transfer system [12]. Due to the double resonance of the signal transmission circuit, the forward and reverse transfer of the signal operate under different resonant frequencies. Since there is no need to attach additional wave traps or inductors, the problem of power transmission loss caused by using wave traps or inductors is solved. We use the amplitude shift keying (ASK) digital modulation approach and analyze the principle of the SS type resonant circuit of the electric energy topology. The problem of large loss of communication signal energy in the additional inductance mode is also avoided, and the communication signal transmission is improved efficiently. Finally, through the parallel transfer of power and signal, we can achieve full duplex communication, minimize the disturbances among power with signal transmission, achieve maximum power transmission and high speed information transmission, while saving system space and cost and better utilizing the advantages of WPT technology.

2. SYSTEM TOPOLOGY

Based on the magnetic coupling wireless power transmission (MC-WPT) system with typical SS structure, this paper connects a signal circuit to a power coupling coil, i.e., the power and signal share a physical channel to realize the shared channel transmission. Fig. 1 displays the circuits topology of power and signal shared channel transmission.

High frequency alternating current is generated by a full-bridge inverter bridge composed of four MOSETs switch tubes, S_1, S_2, S_3, S_4, and then input to the primary power resonance network composed of compensation capacitor C_p and inductor L_p ($L_p = L_{p1} + L_{p2}$). High frequency alternating current is generated in the space near the coupling coil high frequency magnetic field of the same frequency. The electric energy coupling circuit formed by the secondary inductor L_s ($L_s = L_{s1} + L_{s2}$) picks up the electric energy wave, and it becomes DC after the full wave rectification circuit formed by D_1, D_2, D_3, D_4.

Based on the MC-WPT, a part of the electric energy coupling mechanism (L_{p2}, L_{s2}) is used to connect the signal circuit in parallel at both ends to construct a signal channel and realize the two-way transmission of signals. Loosely coupled coils are used on the primary and secondary sides of the signal transmission circuit for signal input. The forward signal is modulated to a high frequency sine wave through a certain modulation method to form a modulated carrier. The electric circuit excites a

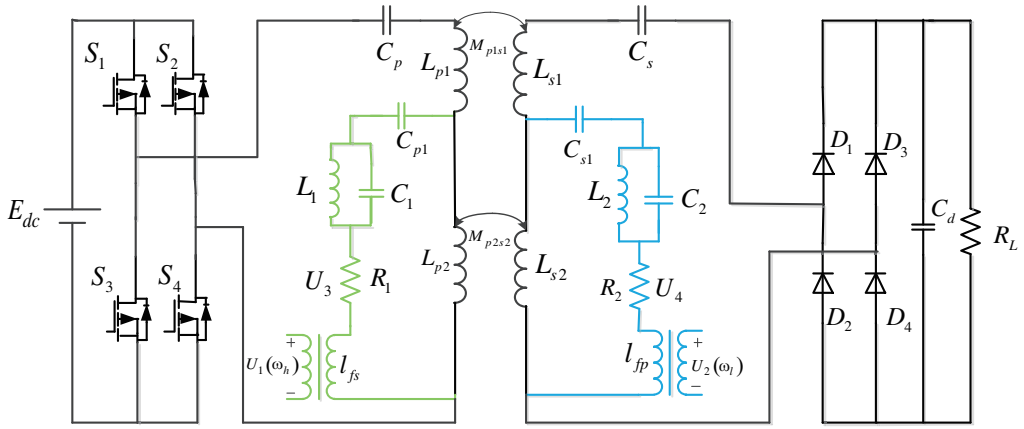

Figure 1. Circuit topology of electric energy and signal transmission.

magnetic field of the same frequency in the adjacent space through part of the electric energy coupling coil L_{p2}. Then the secondary side signal resonant circuit composed of the inductor of the signals matching loop L_{s2} is inductively coupled to the signal carrier transported from the first side of the system. By sampling resistor R_2, the signal waveform with mathematical characteristics is obtained, and the digital signal is demodulated through certain processing (band pass filtering, envelope detection, voltage comparison, etc.) to realize the forward signal wireless transmission. Due to the symmetry of the topology of the signal transmission circuit, the same coupling mechanism is used for both power and signal in order to achieve bidirectional signal transmission. The parallel transfer is done through the same signal resonance network.

During the joint transmission of signal and energy, the circuit design should meet the following requirements to obtain good expected results:

1) The power transmission frequency is much smaller than the signal transmission frequency;
2) $L_{p1} \gg L_{p2}$, $L_{s1} \gg L_{s2}$;

2.1. Analysis of the Characteristics of Electric Energy Network to Signal Wave Resistance

In the MC-WPT system, when the SS structure is adopted, the electric energy resonance network is powered by a voltage source with zero initial resistance of the ideal village. For the topological structure in this paper, looking at signal transmission alone, the equivalent theorem shows that the circuit after high frequency inversion from the DC voltage source is the same as a short circuit. This equivalence circuit is displayed in Fig. 2.

The distribution of the resonant network coupling coil is as follows:

$$\begin{cases} L_{p1} = \alpha L_{p2} \, (\alpha > 10) \\ L_{s1} = \beta L_{s2} \, (\beta > 10) \end{cases} \tag{1}$$

Taking the primary side power transmission network as an example, for some power transmission networks, the impedance Z of that forward transfer network is:

$$Z = j\omega_0 L_{p1} + \frac{1}{j\omega_0 C_p} \tag{2}$$

where ω_0 is the angular frequency of the power transmission system.

When the signal transmits through partial inductance L_{p1} on the electrical energy network, its impedance Z_r is expressed as:

$$Z_r = \frac{1 - \omega^2 L_{p1} C_p}{j\omega C_p} \tag{3}$$

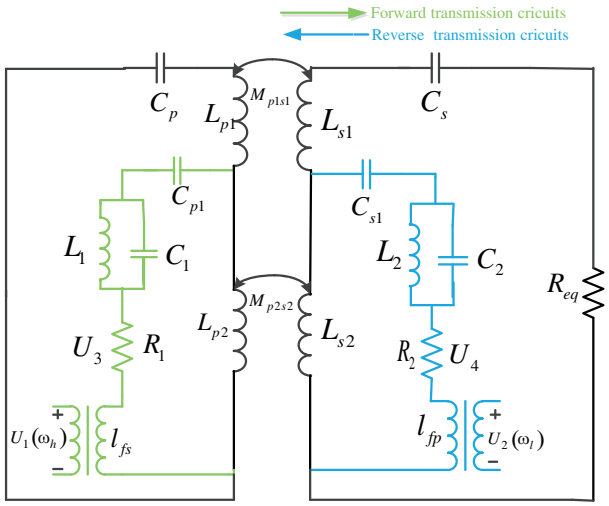

Figure 2. Power trap characteristic circuit.

Because the signal transmission angular frequency ω is much greater than the power transmission angular frequency ω_0, L_p is approximately equal to L_{p1}, that is, $\omega^2 L_{p1} C_p$ much greater than 1, simplify Eq. (3) to get:

$$Z_r \approx \omega L_{p1} \tag{4}$$

Since the signal transmission frequency is much larger than the working frequency of electrical power, a part of electric energy resonance networks have a large impedance to the signal carrier. Because of the synchronous nature of the power transfer loop, the secondary side power transmission circuit also exhibits high impedance characteristics for signal transmission. Part of the power resonance network attenuates the signal carrier greatly, which can inhibit the signal carrier from entering the power transmission network, avoiding the impact on the quality of power transmission. During signal transmission, because of the high impedance effect of the first and second electric energy resonance networks on the signal carrier, it is equivalent to a circuit break for the signal carrier. In other words, it plays the role of high frequency wave blocking, realizing the physical isolation of the power transfer circuits and signal transmission circuit, and reducing the adverse effects of power transfer circuits on signal transmission. As a part of the electrical energy resonance network is also used as a part of the electrical energy transmission channel, that is, it participates in the transmission of electrical energy and has the effect of suppressing the crosstalk between electrical energy and signal, and there is no need to add an additional wave blocking circuit, thereby simplifying the circuit structure of the system.

2.2. Analysis of the Influence of Signal Network on Electric Energy Transmission

When the influence of electrical energy on signal transmission is analyzed, the signal source is equivalent to a short circuit, and the signal coupling inductance value is very small. The structure diagram is simplified as shown in Fig. 3.

Compensation capacitor C_{p1}, parallel inductor L_1, capacitor C_1, and L_{p2} form a resonant network for forward transmission; C_{p1} is at pF level; R_1 is a compensation resistor for forward transmission which is used to alleviate the sudden change caused by the capacitance and inductance, and it is also the reverse transmission of the signal extract resistance. Because the reverse signal transmission circuit is the same, the impedance Z_{rp} of the positive signal transfer circuit and the negative signal transfer impedance Z_{rs} are:

$$\begin{cases} Z_{rp} = \dfrac{j\omega L_1}{1-\omega^2 L_1 C_1} + \dfrac{1}{j\omega C_{p1}} + j\omega l_{fs} + R_1 \\ Z_{rs} = \dfrac{j\omega L_2}{1-\omega^2 L_2 C_2} + \dfrac{1}{j\omega C_{s1}} + j\omega l_{fp} + R_2 \end{cases} \tag{5}$$

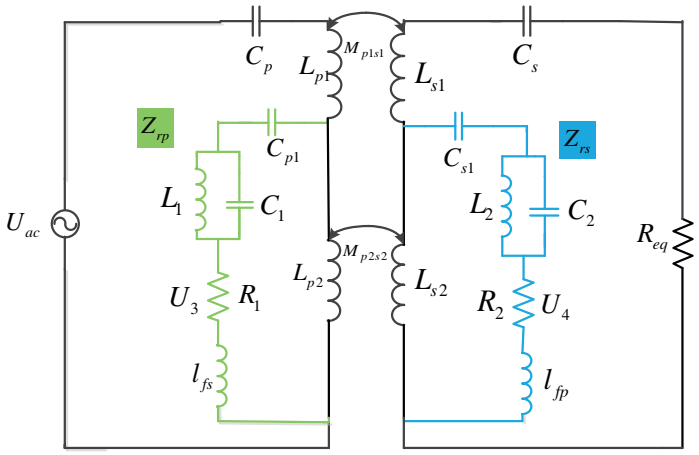

Figure 3. Power transmission impedance analysis circuit.

When electric energy transmission is carried out, the total resistances of the first and second coils are denoted by Z_p and Z_s, respectively:

$$\begin{cases} Z_p = j\omega L_{p1} + \dfrac{1}{j\omega C_p} + \dfrac{j\omega L_{p2} Z_{rp}}{j\omega L_{p2} + Z_{rp}} \\ Z_s = j\omega L_{s1} + \dfrac{1}{j\omega C_s} + \dfrac{j\omega L_{s2} Z_{rs}}{j\omega L_{s2} + Z_{rs}} + R_{eq} \end{cases} \tag{6}$$

The signal transmission frequency is at MHz level and the power transmission frequency at kHz level. The power transmission frequency is very small compared to the signal transmission frequency. Therefore, the resistance values of Z_{rp} and Z_{rs} are very large at the power transfer frequency, which is the same as an opening network. Therefore, Eq. (6) can be equivalent to:

$$\begin{cases} Z_p = \dfrac{1}{j\omega C_p} + j\omega L_{p1} + j\omega L_{p2} \\ Z_s = \dfrac{1}{j\omega C_s} + j\omega L_{s1} + j\omega L_{s2} + R_{eq} \end{cases} \tag{7}$$

After the above analysis, the addition of the signal network has almost no influence on the power transfer, and the resonant frequency during power transfer is almost unchanged. At the same time, some signal transmission networks have large impedance values during power transmission, which can attenuate most of the impact of power.

3. SYSTEM PERFORMANCE ANALYSIS

3.1. Power Transmission Analysis

Through Subsection 2.2 analysis, the circuit transmission structure can be simplified as shown in Fig. 4.

In Fig. 4, U_{ac} is the base wave composition of the square wave voltage produced by that inverter circuit; M is the cross-inductance of the power transmission coil; i_p, i_s are the primary and second currents of the power resonant network, respectively; R_{eq} is the rectification link of the secondary side circuit and the equivalent resistance of the load. The internal resistance of the power supply is ignored. Based on [18], the fundamental voltage and the equivalent resistance can be expressed as:

$$\begin{cases} U_{ac} = 2\sqrt{2}U_{in}/\pi \\ R_{eq} = 8R_L/\pi^2 \end{cases} \tag{8}$$

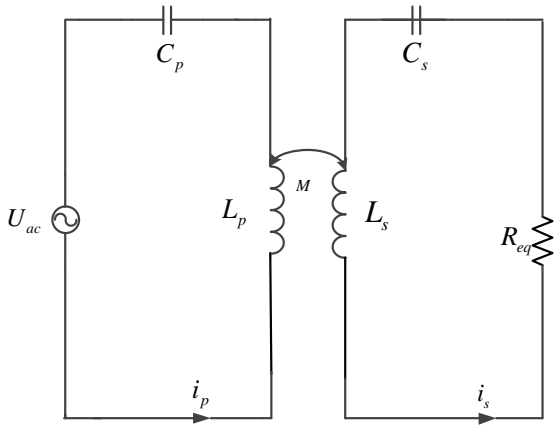

Figure 4. Equal circuit of electric energy transmission.

where U_{in} is the inverter output square wave voltage. According to Kirchhoff's theorem one obtains:

$$\begin{cases} Z_s = j\omega L_s + {}^1\!/_{j\omega C_s} + R_{eq} \\ Z_{sp} = (\omega M)^2 / Z_s \\ Z_p = j\omega L_p + {}^1\!/_{j\omega C_p} + Z_{sp} \\ U_{ac} = i_p Z_p \\ j\omega M i_p = i_s Z_s \\ U_{Req} = i_s R_{eq} \end{cases} \tag{9}$$

where Z_s and Z_p are the impedance of the second and first sides of the power transmission respectively; U_{Req} is the load resistance voltage; and Z_{sp} is the reflected impedance at the second and first sides.

In purpose of improving the system's energy transmission ability and transmission efficiency, both the second and first sides should observe the principle of offsetting inductive impedance and capacitive impedance, that is, reach the resonance state. In this case, the impedances of the second and first sides are purely resistive, which can dramatically improve the power transmission capability. The circuit is in resonance at the angular frequency ω_0, that is:

$$\begin{cases} \omega_0 L_p = {}^1\!/_{\omega_0 C_p} \\ \omega_0 L_s = {}^1\!/_{\omega_0 C_s} \end{cases} \tag{10}$$

Substituting Eq. (10) into Eq. (9) we can obtain:

$$\begin{cases} i_p = U_{ac} R_{eq} / (\omega_0 M)^2 \\ \omega_0 M i_p = i_s R_{eq} \end{cases} \tag{11}$$

According to the above analysis, the voltage gain of the power transmission system G_v can be obtained as:

$$G_v = \left| \frac{U_{Req}}{U_{ac}} \right| = \frac{8R_L}{\pi^2 \omega_0 M} \tag{12}$$

3.2. Analysis of Signal Transfer

Based on the above discussion, when performing signal transmission, some power transmission circuits have extremely high impedance, which corresponds to an opening road and has a negligible effect on the signal circuit. Taking the forward signal circuit as an example, the positive signal transfer circuit diagram is simplified as shown in Fig. 5.

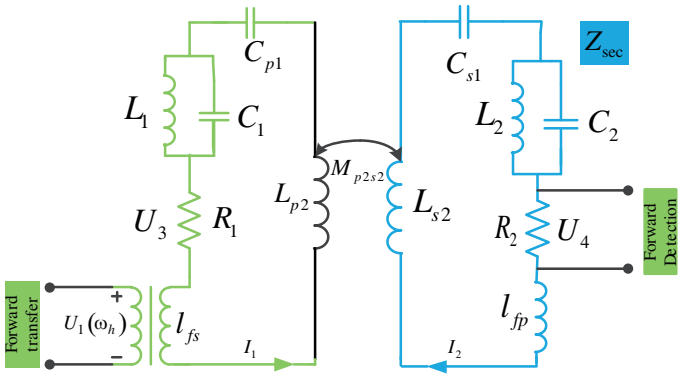

Figure 5. Equivalent model of the positive signal transfer.

M_{p2s2} is the mutual inductance of coupled inductance L_{s2} and L_{p2}. Z_{sec} is the global impedance of the second circuit, and its expression can be derived:

$$\begin{cases} L'_{s2} = L_{s2} + l_{fp} \\ L'_{p2} = L_{p2} + l_{fs} \end{cases} \tag{13}$$

$$Z_{\text{sec}} = \frac{j\omega L_2}{1 - \omega^2 L_2 C_2} + j\omega L'_{s2} + \frac{1}{j\omega C_{s1}} + R_2 \tag{14}$$

According to Eq. (14), the impedance characteristic is illustrated in Fig. 6. It was clearly seen that the impedance values at two frequency points of the circuit are very small. Therefore, the two frequency points f_l and f_h are used as the signal transmission frequency. At these frequency points, the global resistance is the smallest, which is purely resistive.

Let the imaginary part of Z_{sec} be zero, the corresponding resonant points angular frequency can

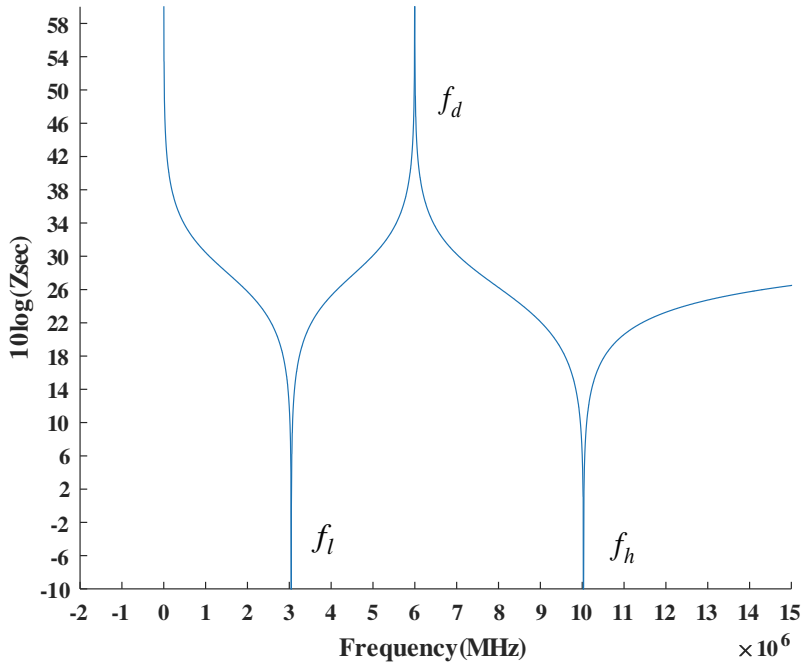

Figure 6. Impedance frequency response.

be obtained as:

$$\begin{cases} \omega_l = \sqrt{\dfrac{L_2C_{s1} + L'_{s2}C_{s1} + L_2C_2 - \sqrt{\left(L_2C_{s1} + L'_{s2}C_{s1} + L_2C_2\right)^2 - 4L'_{s2}C_{s1}L_2C_2}}{2L'_{s2}C_{s1}L_2C_2}} \\ \omega_h = \sqrt{\dfrac{L_2C_{s1} + L'_{s2}C_{s1} + L_2C_2 + \sqrt{\left(L_2C_{s1} + L'_{s2}C_{s1} + L_2C_2\right)^2 - 4L'_{s2}C_{s1}L_2C_2}}{2L'_{s2}C_{s1}L_2C_2}} \\ \omega_d = \dfrac{1}{\sqrt{L_2C_2}} \end{cases} \tag{15}$$

In this paper, the forward transmission frequency is set to f_h, because the forward and reverse structures and parameters are the same, and only the forward transfer circuit is analyzed here.

The impedances of the signal transmission circuit in Fig. 5 are:

$$\begin{cases} Z_{\text{sec}} = \dfrac{j\omega L_2}{1 - \omega^2 L_2C_2} + j\omega L'_{s2} + \dfrac{1}{j\omega C_{s1}} + R_2 \\ Z_{21} = \dfrac{\omega^2 M^2_{p2s2}}{Z_{\text{sec}}} \\ Z_{pec} = \dfrac{j\omega L_1}{1 - \omega^2 L_1C_1} + j\omega L'_{p2} + \dfrac{1}{j\omega C_{p1}} + R_1 + Z_{21} \end{cases} \tag{16}$$

where Z_{21} is the reflected impedance at the second and first sides, and Z_{pec} is the global impedance on the first side. From Eq. (16), the currents on both sides of that circuit and the voltage on the sampling resistor can be obtained as:

$$\begin{cases} I_1 = \dfrac{U_1}{Z_{pec}(\omega_h)} \\ I_2 = \dfrac{j\omega_h M_{p2s2} I_1}{Z_{sec}(\omega_h)} \\ U_4 = I_2R_2 \end{cases} \tag{17}$$

where I_1 is the first side current, I_2 the second side current, and U_4 the voltage on the secondary side sampling resistance. When the signal is transmitted from the forward direction, the sampling voltage is obtained on the sampling resistance. Thus, the information has transmitted successively from the primary coil to the secondary coil. The forward voltage gain G_1 can be obtained as:

$$G_1 = \frac{U_4}{U_1} = \frac{\omega_h M_{p2s2} R_2}{Z_{\text{sec}}(\omega_h) Z_{pec}(\omega_h)} \tag{18}$$

In a similar pattern, while the data is transported from the secondary side, the sampling voltage U_3 is obtained in the sampling resistor R_1, and the backward voltage gain G_2 can be obtained as:

$$G_2 = \frac{U_3}{U_2} = \frac{\omega_l M_{p2s2} R_1}{Z_{\text{sec}}(\omega_l) Z_{pec}(\omega_l)} \tag{19}$$

3.3. Crosstalk Analysis

Because we connect the signal transmission circuit in parallel to the power transmission coupling coil, part of the energy is transferred to the data transfer circuit during energy transmission. The equivalent circuit is modeled in Fig. 7. We can see that in addition to the main side coil, the influence is also the magnetic field interference generated by the side-coil. M_{p1s2} is the mutual inductance between the inductances L_{p1} and L_{s2}, and M_{s1s2} is the mutual inductance between the inductances L_{s1} and L_{s2}.

Using the positive signal transfer for instance, for simple analysis, we ignore the signal circuit, and its corresponding topology is presented in Fig. 8.

According to Fig. 8, the disturbance voltage transmitted to the signal reception network can be acquired as follows:

$$e_{pss2} = j\omega_0 M_{p1s2} i_p - j\omega_0 M_{s1s2} i_s \tag{20}$$

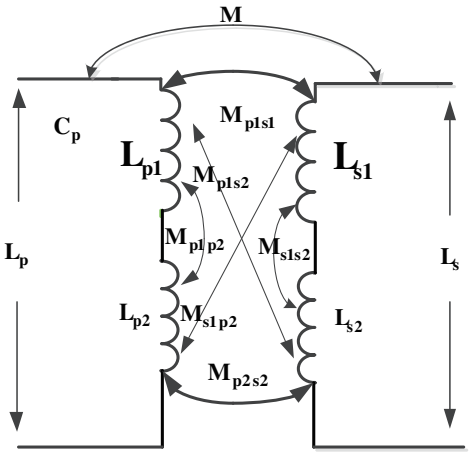

Figure 7. Coupling coil mutual inductance.

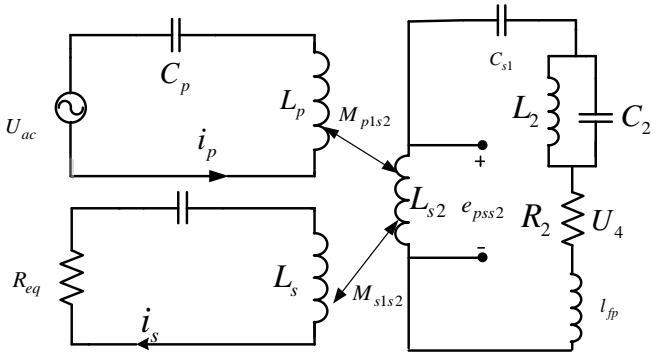

Figure 8. Equivalence module of the disturbance of power transfer to the signal.

By the superposition theorem, the interference voltage on the sampling resistor of the forward signal transmission can be obtained by Eqs. (11) and (20):

$$U_4(\omega_0) = \frac{U_{ac}R_2\left(\frac{8R_L M_{p1s2}}{\pi^2} - \omega_0 M M_{s1s2}\right)}{\omega_0 M^2 Z_{\text{sec}}} \tag{21}$$

Therefore, through Eqs. (17) and (21), the signal to noise ratio of forward signal transfer SNR_f is obtained as follows:

$$SNR_f = 20\lg\frac{U_4(f_h)}{U_4(f_0)} \tag{22}$$

Similarly, the signal to noise ratio of signal backward transfer SNR_r is defined as:

$$SNR_r = 20\lg\frac{U_2(f_l)}{U_2(f_0)} \tag{23}$$

The SNR is an important criterion for measuring the quality of a signal. It can be analyzed from the SNR formula that the input voltage of electric energy should not be too large, and the load resistance should be appropriately small. These phenomena will be analyzed below.

4. MODULATION AND DEMODULATION

2ASK is one of the signal modulation methods in a wireless power and data synchronization transfer network based on the shared channel. It uses the carrier amplitude change to transmit the digital signal,

and its frequency and initial phase remain unchanged, that is, the digital "0" and "1" respectively correspond to different amplitudes. Due to the strengths of simple design, low cost, and high reliability, the OOK scheme is used in this paper. The expression is as follows:

$$f(t) = \begin{cases} A\sin(\omega t) & bit = \text{“1”} \\ 0 & bit = \text{“0”} \end{cases} \tag{24}$$

The signal network based on 2ASK modulation has obvious voltage amplitude changes, and the signal demodulation process adopts non-coherent demodulation. The data demodulation module is primarily composed of a band-pass filter, an envelope detector, and a hysteresis voltage comparator. The voltage on the sampling resistor first passes through the bandpass filter, and then enters the envelope detection road to obtain the envelope voltage waveform of the signal. Finally, the voltage comparator is used to reshape the signal envelope and recover the fundamental band signal. The data demodulation circuit is presented in Fig. 9.

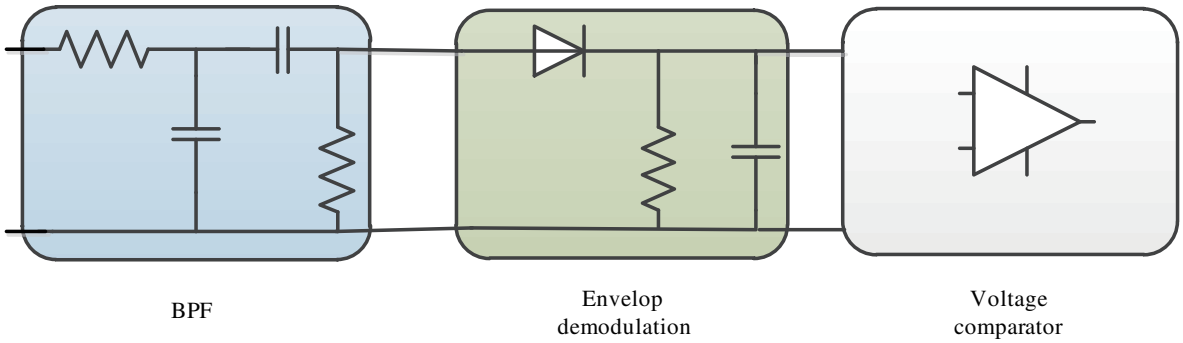

Figure 9. Signal demodulation circuit.

5. SIMULATION VERIFICATION

The system simulation model based on MATLAB/Simulink software was verified, and the transmission characteristics were compared and analyzed through BODE diagram and spectrum analysis diagram.

For the circuit structure proposed in this paper, the values of components and voltages used, and the specific parameter values are shown in Table 1.

Table 1. System parameters.

Parameter	Value	Parameter	Value
E_{dc}	100 V	C_p, C_s	41.74 nF
L_p, L_s	108 µH	C_{p1}, C_{s1}	130 pF
L_{p2}, L_{s2}	8 µH	C_1, C_2	70.4 pF
L_1, L_2	10 µH	f_l	3 MHz
f_0	75 KHz	f_h	10 MHz
M	18 µH	R_1, R_2	300 Ω
M_{p2s2}	2 µH	R_L	20 Ω
U_1, U_2	5 V		

Figure 10 shows the Bode plots of power transfer at different load resistances. We can see from Fig. 10 that with increasing load resistance, the voltage gain gradually increases, which is consistent with the analysis result of Eq. (12). From Fig. 11, with the increase of load resistance, the attenuation of the signal transmission circuit on the electrical power becomes smaller, which will have a larger influence

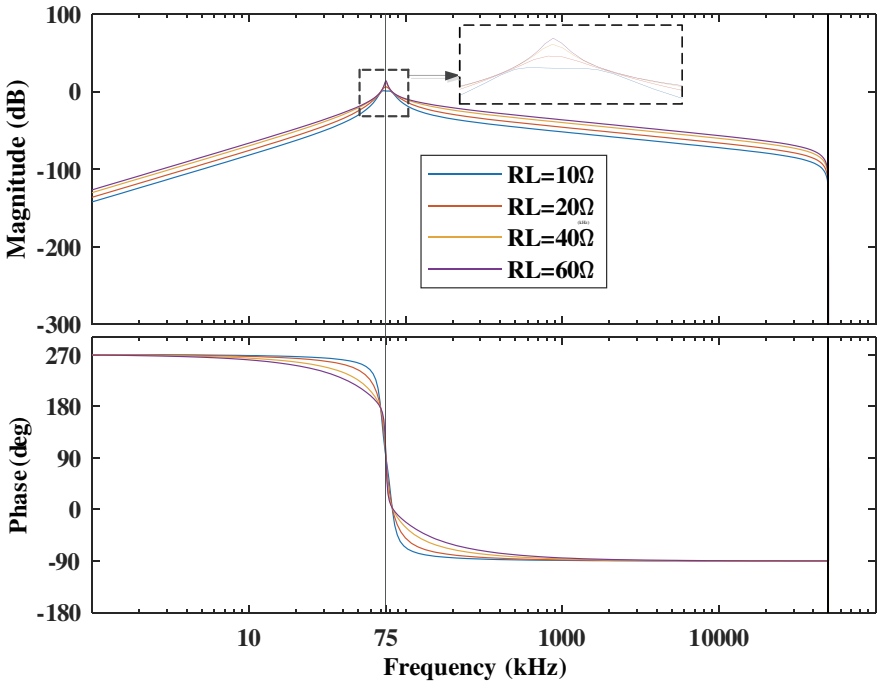

Figure 10. Bode diagram of power transmission under different loads.

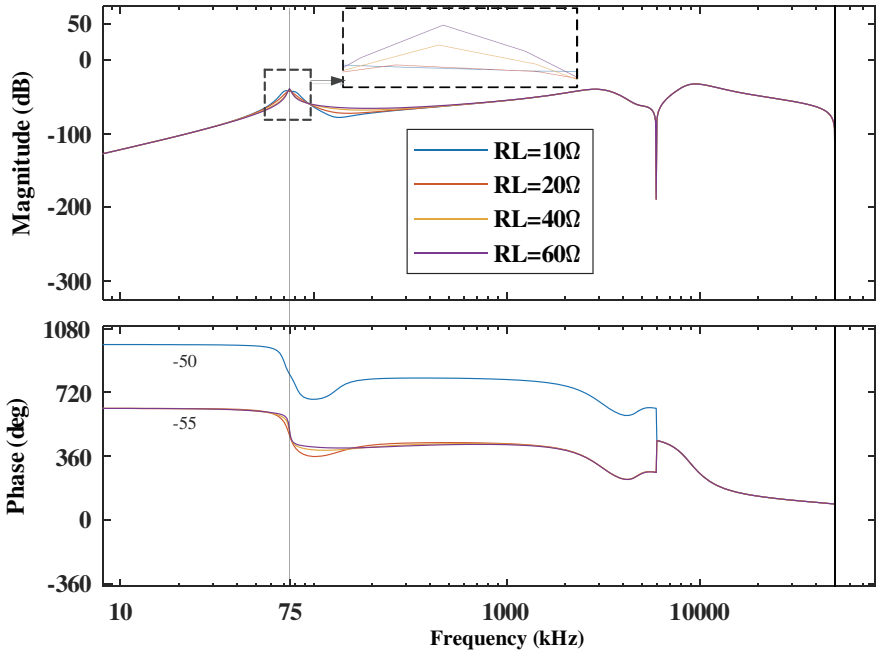

Figure 11. Bode diagram of power attenuation by signal transmission circuit under different loads.

on the signal demodulation. From Eq. (21), we can also see that the interference voltage increases with the growth of the load, so that the SNR becomes smaller, which seriously affects the recovery of the signal.

Figure 12 shows the square wave voltage output by the inverter, the current of the circuit, and the voltage on the load resistor when the input voltage is 100 V. When the load resistance is 20 Ω, the

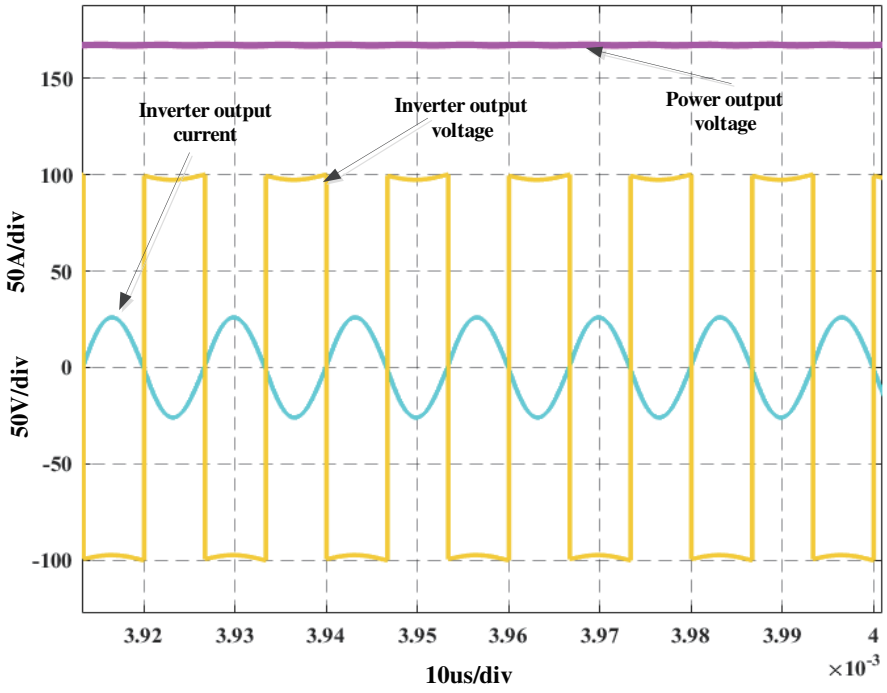

Figure 12. Power transmission waveform.

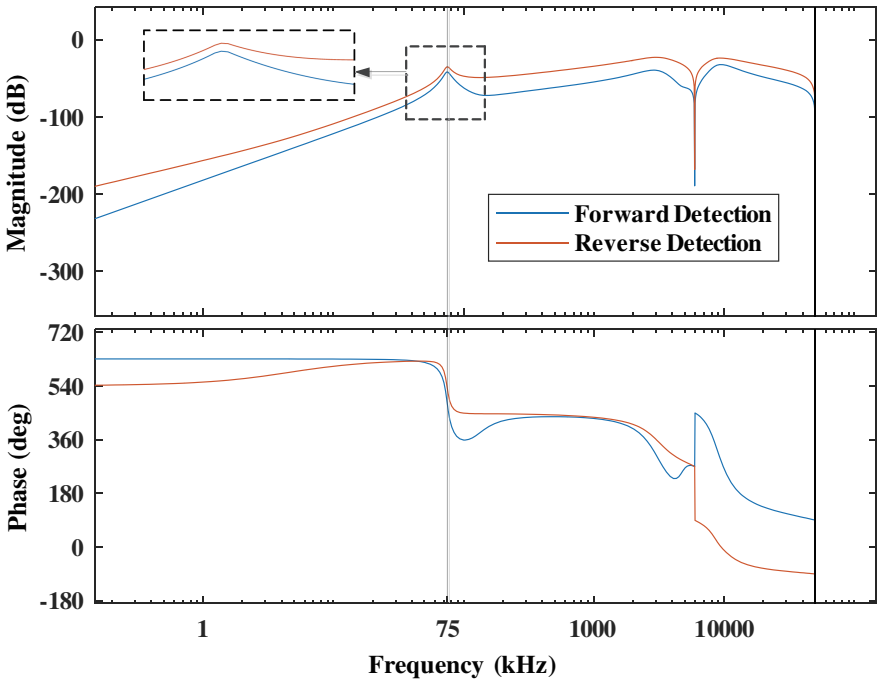

Figure 13. Bode diagram of power transmission on the signal channel.

average value of the resistance voltage is 167.2 V, and the output power is 1.39 KW.

As shown in Fig. 13, for the analysis of the effect of power transmission on signals, the Bode diagram of load resistance of signal transmission circuit on primary side and secondary side is obtained during power transmission. From the attenuation Bode curve, the interference of electric energy transmission

on data transmission is seriously weakened. 1) Data positive transfer procedure: the magnitude of the interference channel is attenuated between 35 $\sim$ 70 dB in the 50 kHz $\sim$ 500 kHz frequency band; 2) The signal reverse transfer procedure: the magnitude of the interference channel in the 1 kHz $\sim$ 500 kHz frequency band the attenuation is between 40 $\sim$ 60 dB. From the above quantitative analysis, we can

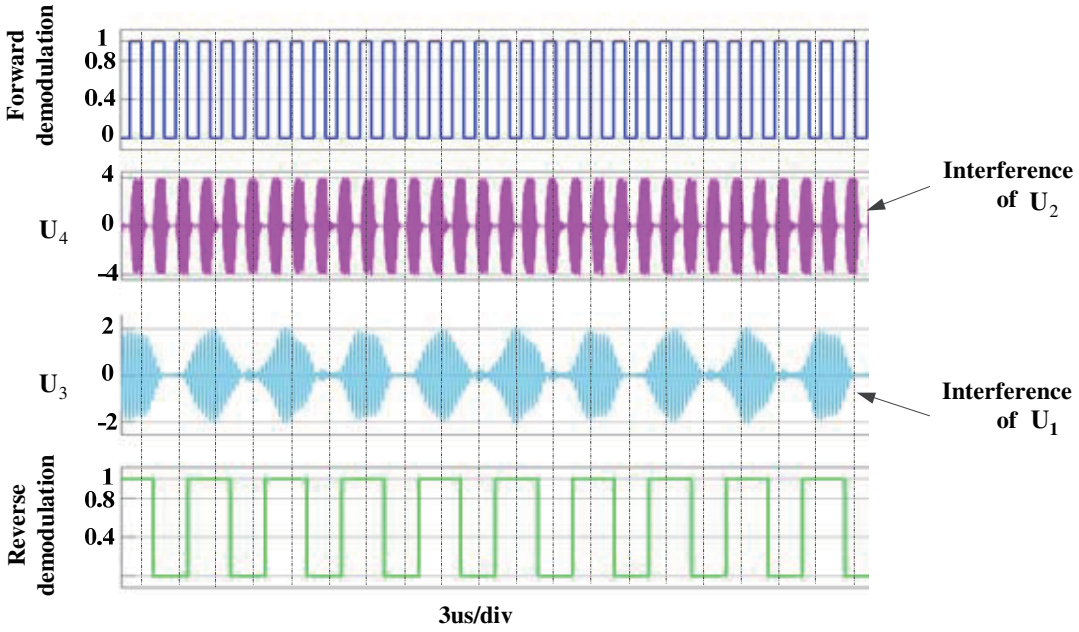

(a)

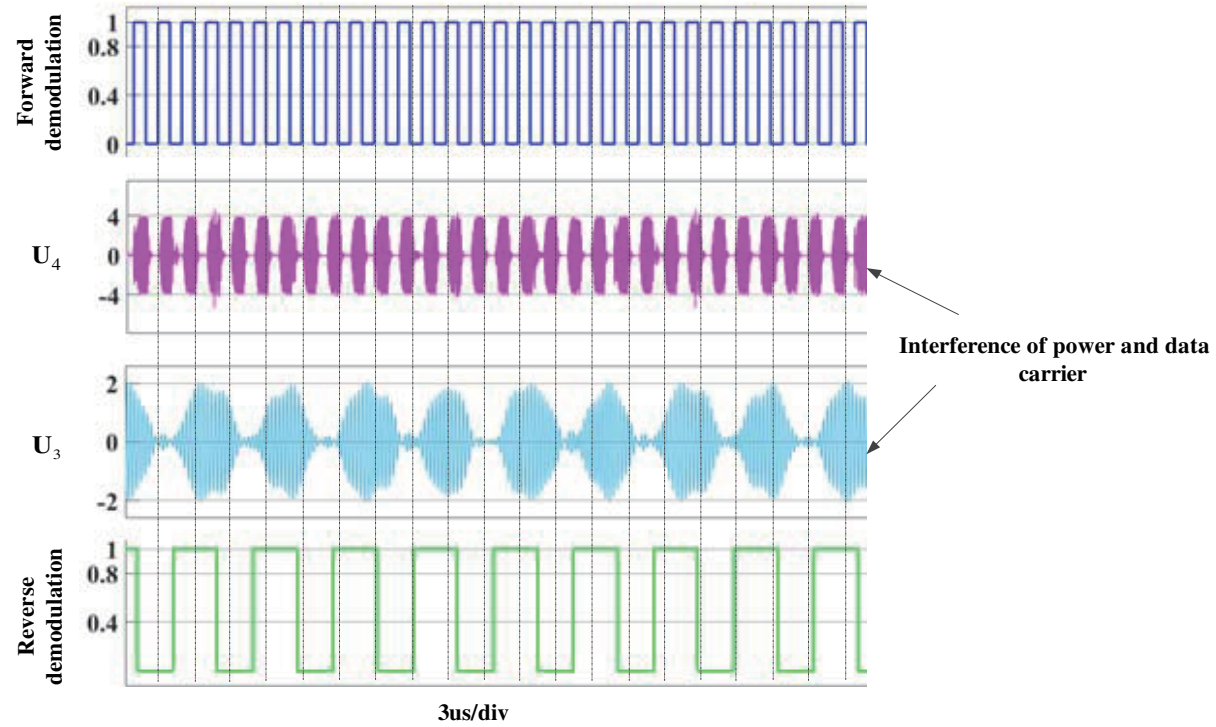

(b)

Figure 14. Waveform of signal transmission channel. (a) No power transmission. (b) Simultaneous transmission of signal and power.

see that the data transmission channel can almost eliminate the influence of a large part of the electric power wave. Secondly, by the band-pass filter, the influence of the remaining part of the electric energy can be eliminated. Although the attenuation performance of interference channel in reverse transmission is a little different from that in forward transmission, the channel from the inverter output to the data pick-up end will greatly weaken the power wave. In other words, the interference of power transmission on data transmission can be ignored through the system parameter design, which verifies the correctness of our previous theoretical analysis.

Figure 14 shows the signal waveform diagram without/with power transmission. Fig. 14(a) is the waveform diagram obtained by band-pass filtering on the sampling resistor when the forward and reverse signals are transmitted at the same time. After the filter circuit, the two-way signal can be separated well, and finally reshaped by the voltage comparator to recover the original signals. Fig. 14(b) is the waveform obtained by the simultaneous transmission of signal and electric energy. We can see that the electric energy signal still has a certain influence on the signal transmission.

The spectrum analysis results of the sampled voltages of the initial and second coils after the band-pass filter are presented in Fig. 15. In the initial coils, the 10 MHz data carrier and power carrier are well suppressed, while in the secondary coil, the 3 MHz data carriers and power carriers are suppressed. From Fig. 15(a) and Fig. 15(b), the total harmonic distortion (THD) of 3 MHz signal transmission is relatively small, because in the system signal modulation process, this link may introduce switching noise and reduce the waveform quality. If the signal speed is too fast, the "concave" or "convex" waveform will be introduced more frequently at the instant of frequency switching, which will adversely affect the quality of the waveform.

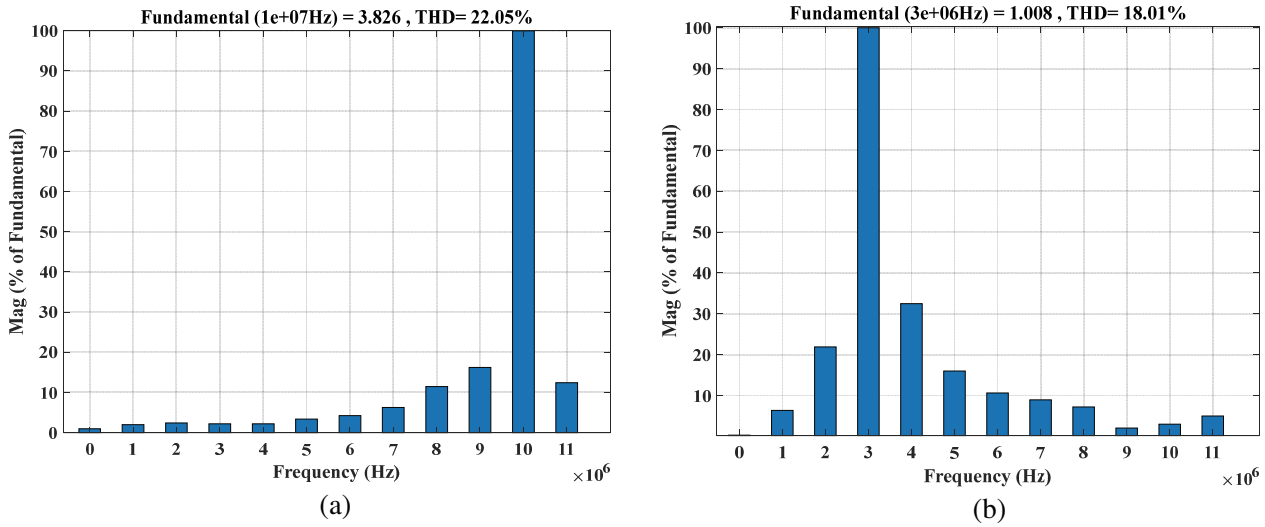

Figure 15. Simultaneous transmission of electric energy and signal carrier. (a) FFT analysis of secondary sampling signal. (b) FFT analysis of primary sampling signal.

6. CONCLUSION

In this paper, a new communication structure of synchronous full-duplex communication and power transfer approaches is proposed, and the practicality of the approach is confirmed by simulation. The signal transmission channel based on partially coupled coils not only improves data transfer rates, but also omits the trap circuit, saving structural space. In addition, this paper analyzes the system performance and the crosstalk between power transmission and data transmission. Experimental results show that forward data can be transmitted at a baud rate of 1 Mbps.

ACKNOWLEDGMENT

This work was supported by the National Natural Science Foundation of China (Grant No. 51877151) and the Program for Innovative Research Team in University of Tianjin (Grant No. TD13-5040).

REFERENCES

1. Cheng, C., Z. Zhou, W. Li, C. Zhu, Z. Deng, and C. C. Mi, "A multi-load wireless power transfer system with series-parallel-series (SPS) compensation," *IEEE Transactions on Power Electronics*, Vol. 34, No. 8, 7126–7130, 2019.
2. Guo, J., L. Tan, H. Liu, W. Wang, and X. Huang, "Stabilization control of output power in double-source wireless power transfer systems without direct output feedback," *IEEE Microwave and Wireless Components Letters: A Publication of the IEEE Microwave Theory and Techniques Society*, Vol. 26, No. 11, 960–962, 2016.
3. Zhao, L., D. Thrimawithana, and U. Madawala, "A hybrid bi-directional wireless EV charging system tolerant to pad misalignment," *IEEE Transactions on Industrial Electronics*, Vol. 64, No. 9, 7079–7086, 2017.
4. Mai, R., Y. Chen, Y. Li, Y. Zhang, G. Cao, and Z. He, "Inductive power transfer for massive electric bicycles charging based on hybrid topology switching with a single inverter," *IEEE Transactions on Power Electronics*, Vol. 32, No. 8, 5897–5906, 2017.
5. Zhou, S. and C. C. Mi, "Multi-paralleled LCC reactive power compensation networks and its tuning method for electric vehicle dynamic wireless charging," *IEEE Transactions on Industrial Electronics*, Vol. 63, No. 10, 6546–6556, 2016.
6. Zhen, Z., K. T. Chau, C. Liu, and C. Qiu, "Energy-security-based contactless battery charging system for roadway-powered electric vehicles," *IEEE PELS Workshop on Emerging Technologies: Wireless Power (2015 WoW). IEEE*, 1–6, 2015.
7. Kilinc, E. G., C. Baj-Rossi, S. Ghoreishizadeh, S. Riario, F. Stradolini, C. Boero, and C. Dehollain, "A system for wireless power transfer and data communication of long-term bio-monitoring," *IEEE Sensors Journal*, Vol. 15, No. 11, 6559–6569, 2015.
8. Esteban, B., M. Sid-Ahmed, and N. C. Kar, "A comparative study of power supply architectures in wireless EV charging systems," *IEEE Transactions on Power Electronics*, Vol. 30, No. 11, 6408–6422, 2015.
9. Li, X., C. Tang, X. Dai, P. Deng, and Y. Su, "An inductive and capacitive combined parallel transmission of power and data for wireless power transfer systems," *IEEE Transactions on Power Electronics*, Vol. 33, No. 6, 4980–4991, 2018.
10. Cen, L., S. N. Melkote, J. Castle, and H. Appelman, "A wireless force-sensing and model-based approach for enhancement of machining accuracy in robotic milling," *IEEE/ASME Transactions on Mechatronics*, Vol. 21, No. 5, 2227–2235, 2016.
11. Brusamarello, V. J., Y. B. Blauth, R. De. Azambuja, I. Muller, and F. R. de Sousa, "Power transfer with an inductive link and wireless tuning," *IEEE Transactions on Instrumentation & Measurement*, Vol. 62, No. 5, 924–931, 2013.
12. Wu, J., C. Zhao, Z. Lin, J. Du, Y. Hu, and X. He, "Wireless power and data transfer via a common inductive link using frequency division multiplexing," *IEEE Transactions on Industrial Electronics*, Vol. 62, No. 12, 7810–7820, 2015.
13. Qian, Z., R. Wang, Z. Wang, J. Du, J. Wu, and X. He, "Closed-loop control design for WPT system using power and data frequency division multiplexing technique," *2016 IEEE Energy Conversion Congress and Exposition (ECCE). IEEE*, 2017.
14. Sun, Y., P. X. Yan, Z. H. Wang, and Y. Y. Luan, "The parallel transmission of power and data with the shared channel for an inductive power transfer system," *IEEE Transactions on Power Electronics*, Vol. 31, No. 8, 5495–5502, 2016.

15. Kim, J., G. Wei, M. H. Kim, H. S. Ryo, and C. Zhu "A wireless power and information simultaneous transfer technology based on 2FSK modulation using the dual bands of series — parallel combined resonant circuit," *IEEE Transactions on Power Electronics*, Vol. 34, No. 3, 2956–2965, 2018.
16. Ji, L., L. Wang, C. Liao, and S. Li, "Simultaneous wireless power and bidirectional information transmission with a single-coil, dual-resonant structure," *IEEE Transactions on Industrial Electronics*, 4013–4022, 2019.
17. Fan, Y., S. Yue, D. Xin, Z. Zuo, and A. You, "Simultaneous wireless power transfer and full-duplex communication with a single coupling interface," *IEEE Transactions on Power Electronics*, 2020.
18. Zhang, Y., T. Kan, Z. Yan, Y. Mao, Z. Wu, and C. C. Mi, "Modeling and analysis of series-none compensation for wireless power transfer systems with a strong coupling," *IEEE Transactions on Power Electronics*, Vol. 34, No. 2, 2018.